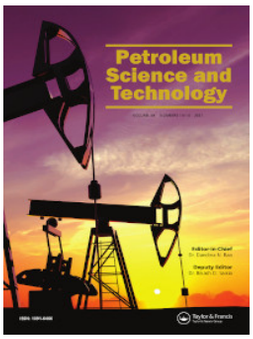

Petroleum Science and Technology

ISSN: (Print) (Online) Journal homepage: https://www.tandfonline.com/loi/lpet20

# Kinetics of thermal decomposition of the polyester nanocomposites

Ercan Aydoğmuş & Hasan Arslanoğlu

**To cite this article:** Ercan Aydoğmuş & Hasan Arslanoğlu (2021) Kinetics of thermal decomposition of the polyester nanocomposites, Petroleum Science and Technology, 39:13-14, 484-500, DOI: 10.1080/10916466.2021.1937218

**To link to this article:** https://doi.org/10.1080/10916466.2021.1937218

PETROLEUM SCIENCE AND TECHNOLOGY
2021, VOL. 39, NOS. 13–14, 484–500
https://doi.org/10.1080/10916466.2021.1937218

Taylor & Francis
Taylor & Francis Group



# Kinetics of thermal decomposition of the polyester nanocomposites

Ercan Aydoğmuş[a] and Hasan Arslanoğlu[b]

[a]Faculty of Engineering, Department of Chemical Engineering, Fırat University, Elazığ, Turkey; [b]Faculty of Engineering and Architecture, Department of Chemical Engineering, Kırşehir Ahi Evran University, Kırşehir, Turkey

**ABSTRACT**

In this study, characterization processes have been done by synthesizing the nano-aerosil-reinforced polyester composite. Chemical bonds formed in polyester composites were examined with FTIR spectrum and thermal stability with proportional integral derivative (PID) system. With the PID system, the drying kinetics of nano-polyester composites were examined from room temperature to 378 K, and thermal decomposition kinetics up to 918 K. The effect of temperature separates volatile components and physical impurities from the structure in the first region. Chemical decomposition starts in the second region, and degradation is the fastest step. Thermal degradation slows in the third region, and the remaining cross-linked components shift away from the structure.

According to the new special solution method, the most suitable function in the thermal decomposition kinetics of polyester nanocomposites was found in the second-order model (f $(\delta) = (1–\delta)^2$, E: 53.492 kJ/mol, $R^2$: 0.99686, for experiment 3). Also, with three-dimensional diffusion and Jander functions have been found better results using Coats-Redfern method ($R^2$: 0.99882, E: 50.55141 kJ/mol for experiment 3). The most consistent results in drying kinetics of polyester nanocomposites were found in the Midilli and Kucuk model ($R^2$: 0.99575, RMSE: 0.03099 for experiment 1).

**KEYWORDS**

aerosil; kinetic model; nanocomposite; polyester; thermal decomposition

## Highlights

- Physico-chemical characterization of Polyester Nano-Composites
- Thermal Decomposition analyses of Polyester Nano-Composites
- Kinetic study using Advanced Iso-conversional & Iso-conversional model
- Thermodynamic parameters of Polyester Nano-Composites

## 1. Introduction

Today, nano-sized additives and fillers give polymers many physical or chemical properties. Depending on the purpose of use, organic or inorganic additives improve the properties desired in polymers. In polymer materials,

CONTACT Hasan Arslanoğlu hasan.arslanoglu@ahievran.edu.tr Faculty of Engineering and Architecture, Department of Chemical Engineering, Kırşehir Ahi Evran University, Kırşehir, Turkey.

properties such as insulation, thermal stability, density, hardness, and porosity are provided by these additives. There are many studies in the literature developed by adding physical and chemical additives according to the intended use of such polymers. The thermal decomposition kinetics of the polypropylene/poly (lactic acid) mixture harmonized with artificial aging (Hayoune et al. 2020) and thermoplastic polyesters have been studied (Levchik and Weil 2004). The thermal decomposition kinetics and decomposition mechanism of metal oxide-filled polyesters (Tibiletti et al. 2011), and furan dicarboxylic acid-based polyesters with low-molecular-weight aliphatic diols (Tsanaktsis et al. 2015), were investigated in the studies.

In studies conducted using biomass, thermal decomposition processes of nanocomposites made with bio-based polyesters (TranVan, Legrand, and Jacquemin 2014) and balsa trees (Terzopoulou et al. 2019) were examined and their thermal degradation behavior was determined. In another study, the kinetics and mechanisms of thermal degradation of a semi-crystalline bio-based polyester with a high-molecular-weight were analyzed and its chemical structure was investigated (Terzopoulou et al. 2016). The effects of different nanoparticles on the thermal decomposition of poly (propylene sebacate)/nanocomposites were evaluated by thermogravimetric analysis (TGA). Correlation coefficients of kinetic model equations were calculated by performing nonlinear regression (Chrissafis et al. 2012).

Decomposition processes are a promising route for plastic waste treatment due to their capability of converting plastic waste into valuable materials that can be used as feedstock for petrochemistry, like monomers or even fuels. The decomposition processes can be run as thermal or catalytic, and it has a lower sensitivity to the composition of the material being processed, in comparison with mechanical recycling. Consequently, it allows the processing of mixed and unwashed plastic wastes. For a suitable design of a decomposition processes reactor, the knowledge of the degradation kinetics is extremely important.

Changes in physical and chemical properties in a study simulated by the disposal of commercial polylactide were evaluated by thermal analysis techniques (Badía et al. 2010). Polyester-based polyurethane is widely used in security and military applications. The thermal stability of these polymers was analyzed with the help of tests such as Thermogravimetric Analysis (TGA) and Differential Scanning Calorimetry (DSC) (Singh et al. 2020). In another study, PET nanocomposite was obtained with modified montmorillonite and fumed silica. It has been observed that the additives in this composite increase the thermal stability (Vassilioua, Chrissafisb, and Bikiaris 2010). The thermal decomposition kinetics of a mixture of polycarbonate, poly (trimethylene terephthalate), and poly (butylene terephthalate) were investigated. Thermal decomposition kinetics of pure polymer and mixtures

were investigated with a thermogravimetric analyzer (TGA) device (Al-Mulla et al. 2011).

Thermal decomposition kinetics of Vectra copolyester with thermotropic poly(oxybenzoate-co-oxynaphthoate) in nitrogen environment were investigated. Activation energy in isothermal thermogravimetric experiments is calculated as 255 kJ/mol on average and 374 kJ/mol in a non-isothermal state (Li and Huang 1999). In a study on thermal degradation, it was determined by theoretical analysis that polymer materials are dependent on many complex dynamic functions. Flynn-Wall-Ozawa method was applied to examine the activation energy of flame-retardant thermoset polylactic acid and it was determined that the activation energy increased slowly (Li et al. 2019). In an article in which aerogel particles were added to epoxy resin, it was determined that both density and thermal conductivity coefficient decreased. The effects of various aerogel particle sizes on the thermal and mechanical properties of epoxy composites were investigated (Kucharek, MacRae, and Yang 2020).

Polymer composites have good mechanical, friction, durability, and wear performance after fumed silica is reinforced (Alameri and Oltulu 2020). Fumed silica particles should be homogeneously dispersed in the nanoscale, unsaturated polyester resin (Rajaee et al. 2019). Ultrasonic wave dispersion method is also used to mix unsaturated polyester resin with fumed silica (Majeed and Ibrahim 2017; Majeed 2018). The polyester composites obtained are used in automobile, building, and aviation industries due to their light weight and high strength (Ahmad et al. 2017). The fumed silica used (aerosil R812S, R805, and R816) and unsaturated polyester can show different mechanical strength. It has been determined that polyester composites have high mechanical strength and chemical resistance in building applications and repair techniques (Singh, Kumar, and Singh 2019). It has been proven by TGA that the thermal stability of aerosil-reinforced polyester composites is improved (Halim et al. 2020; Mourad, Abu-Jdayil, and Hassan 2020).

In the researches, the use of nano-fume silica (aerosil 300), which goes up the thermal stability of the polyester composite, decreases the thermal conductivity coefficient, and goes down the density, has not been studied. Also, there is no study examining both drying and thermal decomposition kinetics of aerosil reinforcement polyester nanocomposites.

Polyester nanocomposite has a lower density, higher thermal stability, and greater thermal insulation due to its aerosil reinforcement, making it ideal for many applications. This study will shed light on the literature in order to improve the desired properties of unsaturated polyesters according to their intended use and to develop new composites.

Table 1. The experimental working plan of the unsaturated polyester and nanocomposites.

| Experiment numbers | Aerosil (wt.%) | Polyester resin (wt.%) | Cobalt octoate (wt.%) | MEKP (wt.%) |
|---|---|---|---|---|
| 1 | 4 | 94 | 0.5 | 1.5 |
| 2 | 3 | 95 | 0.5 | 1.5 |
| 3 | 2 | 96 | 0.5 | 1.5 |
| 4 | 1 | 97 | 0.5 | 1.5 |
| 5 | 0 | 98 | 0.5 | 1.5 |

## 2. Materials and methods

### 2.1 Materials

An experimental study plan for polyester composite can be seen in Table 1. The polyester (TP 100) used here is an orthophthalic-based unsaturated polyester resin. Methyl ethyl ketone peroxide (MEKP, Akperox A1) is used to cure unsaturated polyester resins at room temperature. and usually used in combination with cobalt octoate (Akcobalt KXC6). Aerosil 300 has a surface area of 301.2 $m^2$/g, a particle diameter of 7 nm, a density of 55 kg/$m^3$, and $SiO_2$ content of 99.8%. It is an inorganic substance with very good thermal stability and insulation properties.

### 2.2 Methods

In this study, the drying and thermal decomposition kinetics of aerosil reinforcement thermoplastic polyester have been investigated. First, pure polyester was prepared and aerosil of nano-size was added in certain proportions. After adding a certain amount of MEKP and cobalt octoate to the mixture, the exothermic reaction has waited for completion. There is both chemical reaction and physical interaction of aerosil particles in the obtained nanocomposite. To determine the thermal stability of this composite, volatile components were removed by drying first, and then, the decomposition behavior in an inert environment was investigated with a proportional integral derivative (PID) controlled system (Figure 1). Thermal decomposition experiments were performed with the PID system in non-isothermal conditions from room temperature to 918 K with a temperature increase of 10 K/min. In order to fully comprehend the thermal decomposition kinetics of polyester composite, it has been evaluated as optimum to operate at 10 K/min heating rate in PID system. It takes a lot of time to operate at lower heating rates and the high-temperature increase cannot be analyzed well quantitatively and qualitatively in the thermal decomposition zones in the PID system

## 3. Result and discussion

### 3.1 Special mathematical solution for kinetic modeling

Thermal decomposition kinetics are thermogravimetrically based on the mathematical study of the effect of the lost mass on transformation (Table 2).

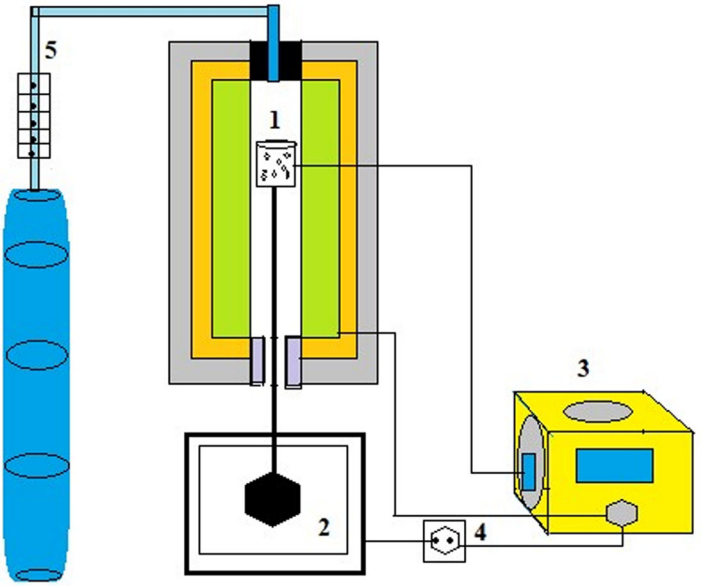


**Figure 1.** PID experimental system: thermal decomposition cell (1), electronic mass scale (2), potentiometer and PID control system (3), electric source (4), nitrogen tube and flow meter (5).

The solution of the reaction rate constant $k(t,T)$, which is a function of time or temperature, with a function $f(\delta)$ depending on the transformation is given below. Since temperature is also a function of time, it can be expressed as $T(t) = \alpha t$. In experimental studies, the rate of temperature increase can be written as $\alpha = 10\,\mathrm{K/min}$.

In model equations: $M_t$ is the mass at time $t$, $M_i$ is the initial mass, and $M_\infty$ is the final mass. $\delta$ is the conversion ratio, $k(T)$ is the temperature-dependent function, and $f(\delta)$ is the conversion-dependent function (White, Catallo, and Legendre 2011).

$$\delta = \frac{M_t - M_\infty}{M_i - M_\infty} \tag{1}$$

$$\frac{d\delta}{dt} = k(T)f(\delta) \tag{2}$$

$$f(\delta) = \delta^m(1-\delta)^n \tag{3}$$

$$dT = \alpha dt \tag{4}$$

$$k(T) = (\xi + \beta T^\eta) \tag{5}$$

$$\frac{d\delta}{dT} = \frac{1}{\alpha}(\xi + \beta T^\eta)\delta^m(1-\delta)^n \tag{6}$$

$$k(T) = \frac{\delta}{\delta^m(1-\delta)^\eta} = \frac{T(\xi + \beta T^\eta + \xi\eta)}{\alpha(\eta+1)} \tag{7}$$

**Table 2.** Special solutions for the kinetic models ($\delta \neq 1$).

| Numbers | Kinetic models | f($\delta$) | $k(T) = \frac{T(\xi+\beta T^{\eta}+\xi\eta)}{\alpha(\eta+1)}$ |
|---|---|---|---|
| 1 | Avrami-Erofe | $2(1-\delta)[-\ln(1-\delta)]^{1/2}$ | $k(T) = \frac{\delta}{2(1-\delta)(-\ln(1-\delta))^{1/2}}$ |
| 2 | Avrami-Erofe | $3(1-\delta)[-\ln(1-\delta)]^{2/3}$ | $k(T) = \frac{\delta}{3(1-\delta)(-\ln(1-\delta))^{2/3}}$ |
| | | | $3Ta(-\ln(1-\alpha))^{2/3}(\frac{b}{T})^{C}(\alpha-1)/(c-1)$ |
| 3 | Avrami-Erofe | $4(1-\delta)[-\ln(1-\delta)]^{3/4}$ | $k(T) = \frac{\delta}{4(1-\delta)(-\ln(1-\delta))^{3/4}}$ |
| 4 | One-dimensional diffusion | $1/(2\delta^{-1})$ | $k(T) = 2$ |
| 5 | Two-dimensional diffusion | $[-\ln(1-\delta)]^{-1}$ | $k(T) = -\delta\ln(1-\delta)$ |
| 6 | Three-dimensional diffusion | $(3/2)(1-\delta)^{2/3}[1-(1-\delta)^{1/3}]^{-1}$ | $k(T) = \frac{2\delta[1-(1-\delta)^{1/3}]}{3(1-\delta)^{2/3}}$ |
| 7 | Ginstling-Brounshtein | $(3/2)[(1-\delta)-(1/3)-1]$ | $k(T) = \frac{2[1-(1-\delta)^{1/3}]}{3(1-\delta)^{1/3}}$ |
| 8 | First order | $(1-\delta)$ | $k(T) = \frac{\delta}{(1-\delta)}$ |
| 9 | Second order | $(1-\delta)^2$ | $k(T) = \frac{\delta}{(\delta-1)^2}$ |
| 10 | Third order | $(1-\delta)^3$ | $k(T) = \frac{\delta}{(1-\delta)^3}$ |
| 11 | Parabolic Law | $1/\delta$ | $k(T) = \delta^2$ |
| 12 | Holt-Cutler-Wadsword | $1/-\ln(1-\delta)$ | $k(T) = \delta\ln(\delta-1)$ |
| 13 | Jander | $(1-\delta)^{2/3}/[1-(1-\delta)^{1/3}]$ | $k(T) = \frac{\delta[1-(1-\delta)^{1/3}]}{(1-\delta)^{2/3}}$ |
| 14 | Zhuravlev-Lesokhin-Tempelmen | $(1-\delta)^{5/2}/[1-(1-\delta)^{1/3}]$ | $k(T) = \frac{\delta[1-(1-\delta)^{1/3}]}{(1-\delta)^{5/2}}$ |
| 15 | Komatsu-Uemuro (anti-Jander) | $(1+\delta)^{2/3}/[(1+\delta)^{1/3}-1]$ | $k(T) = \frac{\delta[(1+\delta)^{1/3}-1]}{(1+\delta)^{2/3}}$ |

The thermal decomposition kinetics of polyester composites with the special mathematical solution expressed in Eq. (7) have been calculated with the help of statistical analysis.

### 3.2 Statistical analysis

To investigate the reliability of the results obtained from the models, the most appropriate model was determined by applying statistical tests such as RMSE and chi square in the equations. Root mean square error (RMSE), chi square ($\chi^2$), residual sum of squares (SSR), error sum of squares (SSE), the total sum of squares (SST), and $R^2$ are statistical parameters. In the following equations, experimental data ($M_{ei}$), values in the model ($M_{mi}$), the number of experiments ($N$), the number of parameters in the model ($n$), the average of the values in the model ($M_{\overline{mi}}$), and the average of the data in the experiments ($M_{\overline{ei}}$) were shown. Also, the statistical efficiency ($Ef$) was calculated and the experimental results were compared with the theoretical models (Ott and Longnecker 2001; Phogat et al. 2016).

$$\mathrm{RMSE} = \sqrt{\frac{\sum_{i=1}^{N}(M_{ei} - M_{mi})^2}{N}} \tag{10}$$

$$Ef = \frac{\sum_{i=1}^{N}\left[(M_{ei}-M_{\overline{ei}})^2 - (M_{mi}-M_{ei})^2\right]}{\sum_{i=1}^{N}(M_{ei}-M_{\overline{ei}})^2} \tag{11}$$

**Table 3.** Kinetic models used in regression analysis of the polyester nanocomposites.

| Model number | Model name | Equation |
|---|---|---|
| 1 | Lewis | $M_R = \exp(-kt)$ |
| 2 | Page | $M_R = \exp(-kt^c)$ |
| 3 | Modified Page | $M_R = \exp(-(kt)^c)$ |
| 4 | Henderson ve Pabis | $M_R = (a)\exp(-kt)$ |
| 5 | Logarithmic | $M_R = (a)\exp(-kt)+b$ |
| 6 | Two term | $M_R = (a)\exp(-kt)+ (b)\exp(-ct)$ |
| 7 | Two-term exponential | $M_R = (a)\exp(-kt)+ (1-a)\exp(-akt)$ |
| 8 | Midilli and Kucuk | $M_R = (a)\exp(-kt^b)+ct$ |
| 9 | Diffusion approach | $M_R = (a)\exp(-kt)+ (1-a)\exp(-kbt)$ |
| 10 | Verma et al. | $M_R = (a)\exp(-kt)+ (1-a)\exp(-bt)$ |

$$\chi^2 = \frac{\sum_{i=1}^{N}(M_{ei} - M_{mi})^2}{N - n} \tag{12}$$

$$\mathrm{SSE} = \sum_{i=1}^{N}(M_{ei} - M_{mi})^2 \tag{13}$$

$$\mathrm{SST} = \sum_{i=1}^{N}(M_{ei} - M_{\overline{mi}})^2 \tag{14}$$

$$R^2 = 1 - \frac{SSE}{SST} \tag{15}$$

### 3.3 Nanocomposites drying kinetics

According to the experimental study plan, first the drying kinetics of polyester nanocomposites and then the thermal decomposition kinetics were investigated together. In drying kinetics, physical impurities, that is, the separation of volatile components such as moisture, have been discussed using both experimental and drying kinetic models. The drying process of the polymers at the temperature of 293 K was carried out in non-isothermal conditions with a temperature increase of 10 K/h for a total of 10 h. Volatile components of composites obtained in experimental studies were removed. Using the model equations in Table 3, the drying kinetics of the polyester composite are examined and the correlation coefficients were calculated. In Table 4, the parameters found by nonlinear regression and statistical analysis are written. According to the evaluation of the drying kinetics models obtained in Table 4, Midilli and Kucuk equation for the 1st, 2nd, 4th, and 5th experiments gave more dominant results compared with the other kinetic models. In the third experiment, logarithmic equation gave the most compatible results with the experimental data. In the statistical analysis, the harmony of the theoretical and experimental results was evaluated by examining the maximum $R^2$ and minimum error function (RMSE, SSE, and $\chi^2$) values.

**Table 4.** Model coefficients and statistical analysis of drying kinetics for the polyester and nanocomposites.

| Experiments | Model | $k$ | $a$ | B | $c$ | $R^2$ | RMSE | SSE | $\chi^2$ |
|---|---|---|---|---|---|---|---|---|---|
| 1 | 1 | 0.01872 | | | | 0.95925 | 0.10479 | 0.01985 | 0.00215 |
| | 2 | 0.02025 | | | 0.96045 | 0.96092 | 0.10695 | 0.02013 | 0.00244 |
| | 3 | 0.02350 | | | 1.12425 | 0.95075 | 0.10979 | 0.02535 | 0.00304 |
| | 4 | 0.01912 | 1.00276 | | | 0.95937 | 0.10306 | 0.02010 | 0.00241 |
| | 5 | 0.09442 | 0.28710 | 0.72585 | | 0.97051 | 0.09396 | 0.00889 | 0.00204 |
| | 6 | 0.02290 | 1.01157 | 0.00005 | −0.68266 | 0.98482 | 0.06685 | 0.01153 | 0.00127 |
| | 7 | 0.09624 | 0.11647 | | | 0.96595 | 0.10397 | 0.01759 | 0.00226 |
| | 8 | 0.05359 | 0.99785 | 1.29849 | 0.05062 | 0.99575 | 0.03099 | 0.00267 | 0.00036 |
| | 9 | 0.02018 | 0.99999 | −47.7596 | | 0.96648 | 0.10404 | 0.00959 | 0.00264 |
| | 10 | 0.19260 | 0.02570 | 0.01616 | | 0.96327 | 0.10562 | 0.01025 | 0.00273 |
| 2 | 1 | 0.01194 | | | | 0.98162 | 0.05795 | 0.00398 | 0.00060 |
| | 2 | 0.00859 | | | 1.16399 | 0.98349 | 0.04584 | 0.06541 | 0.00051 |
| | 3 | 0.02183 | | | 1.33121 | 0.97873 | 0.05612 | 0.00846 | 0.00076 |
| | 4 | 0.01284 | 1.00613 | | | 0.98154 | 0.05549 | 0.00656 | 0.00058 |
| | 5 | 0.00246 | 4.98614 | −3.98092 | | 0.98219 | 0.05432 | 0.00709 | 0.00066 |
| | 6 | 0.01284 | 0.66466 | 0.34147 | 0.01284 | 0.98154 | 0.05549 | 0.00974 | 0.00081 |
| | 7 | 0.01194 | 0.99995 | | | 0.98162 | 0.05795 | 0.00711 | 0.00068 |
| | 8 | −0.06989 | 0.99780 | 0.83660 | −0.07248 | 0.98496 | 0.05082 | 0.00682 | 0.00067 |
| | 9 | 0.92039 | −0.01286 | 0.01496 | | 0.98484 | 0.04842 | 0.00614 | 0.00057 |
| | 10 | 0.92057 | −0.01286 | 0.01377 | | 0.98484 | 0.04841 | 0.00609 | 0.00057 |
| 3 | 1 | 0.01066 | | | | 0.95114 | 0.06665 | 0.00106 | 0.00091 |
| | 2 | 0.00915 | | | 1.07611 | 0.95066 | 0.06678 | 0.00118 | 0.00104 |
| | 3 | 0.02181 | | | 1.39432 | 0.93446 | 0.09149 | 0.00226 | 0.00182 |
| | 4 | 0.01110 | 1.00304 | | | 0.95116 | 0.06976 | 0.00989 | 0.00103 |
| | 5 | 0.01762 | 0.65247 | 0.35108 | | 0.97027 | 0.06968 | 0.01086 | 0.00120 |
| | 6 | −0.00552 | 0.66884 | 0.33636 | 0.05290 | 0.94626 | 0.07214 | 0.01499 | 0.00156 |
| | 7 | 0.01066 | 0.99907 | | | 0.95114 | 0.06665 | 0.00993 | 0.00104 |
| | 8 | −0.00176 | 1.00178 | 0.91333 | −0.01197 | 0.95023 | 0.06991 | 0.01354 | 0.00147 |
| | 9 | 0.01066 | 0.78334 | 0.99909 | | 0.95114 | 0.06662 | 0.01147 | 0.00121 |
| | 10 | 1.07522 | −0.00581 | 0.01149 | | 0.95184 | 0.06963 | 0.01125 | 0.00119 |
| 4 | 1 | 0.01052 | | | | 0.97124 | 0.04398 | 0.00494 | 0.00052 |
| | 2 | 0.01131 | | | 0.96355 | 0.97241 | 0.04712 | 0.00603 | 0.00058 |
| | 3 | 0.01931 | | | 1.31132 | 0.94775 | 0.08572 | 0.01552 | 0.00149 |
| | 4 | 0.01055 | 1.00023 | | | 0.97124 | 0.04368 | 0.00587 | 0.00060 |
| | 5 | 0.05786 | 0.22846 | 0.77542 | | 0.97692 | 0.04897 | 0.00559 | 0.00057 |
| | 6 | −0.00627 | 0.66809 | 0.33561 | 0.05415 | 0.97684 | 0.05219 | 0.00681 | 0.00072 |
| | 7 | 0.06602 | 0.09154 | | | 0.97491 | 0.04828 | 0.00496 | 0.00053 |
| | 8 | 0.04057 | 0.99749 | 1.18233 | 0.03699 | 0.98748 | 0.03923 | 0.0412 | 0.00039 |
| | 9 | 0.05256 | 0.28333 | −0.05622 | | 0.97719 | 0.05438 | 0.00593 | 0.00064 |
| | 10 | 0.14797 | 0.03333 | 0.00755 | | 0.97512 | 0.05210 | 0.00647 | 0.00065 |
| 5 | 1 | 0.00919 | | | | 0.92968 | 0.08235 | 0.01099 | 0.00127 |
| | 2 | 0.00551 | | | 1.25371 | 0.93487 | 0.07696 | 0.0987 | 0.00119 |
| | 3 | 0.00825 | | | 0.96600 | 0.92737 | 0.08488 | 0.01378 | 0.00152 |
| | 4 | 0.01014 | 1.00653 | | | 0.92956 | 0.08511 | 0.01151 | 0.00129 |
| | 5 | 0.00089 | 10.95528 | −9.94935 | | 0.93054 | 0.08455 | 0.01505 | 0.00148 |
| | 6 | 0.01014 | 0.52449 | 0.48204 | 0.01013 | 0.92956 | 0.08506 | 0.02041 | 0.00180 |
| | 7 | 0.00919 | 0.99988 | | | 0.92968 | 0.08235 | 0.01567 | 0.00145 |
| | 8 | 0.03182 | 0.99561 | 1.25021 | 0.03457 | 0.95003 | 0.07069 | 0.01228 | 0.00130 |
| | 9 | 0.00919 | 0.81030 | 0.99979 | | 0.92968 | 0.08236 | 0.01842 | 0.00169 |
| | 10 | 0.68670 | −0.01625 | 0.01144 | | 0.93984 | 0.07218 | 0.01684 | 0.00130 |

### *3.4 Thermal decomposition kinetics*

Thermal decomposition kinetics of polyester composites are evaluated in the last section. The special mathematical solution developed here and the activation energy values found in the Coast-Redfern method were calculated. The data in the thermal decomposition experiments have been evaluated with the help of statistical analysis using these two methods.

**Table 5.** Correlation coefficients and statistical analysis of the special solutions.

| Experiment 3 (2wt.%) | | | | | | | | |
|---|---|---|---|---|---|---|---|---|
| Models | $\xi$ | $\beta$ | $\eta$ | $\alpha$ | $R^2$ | RMSE | SSE | $\chi^2$ |
| 1 | −0.30742 | 0.31357 | −0.00352 | 1.37564 | 0.99034 | 0.00136 | 0.00020 | 0.00007 |
| 2 | −0.00554 | 0.13283 | −0.95856 | 10.6521 | 0.99042 | 0.00115 | 0.00012 | 0.00004 |
| 3 | −0.00284 | 0.07775 | −0.66248 | 4.55093 | 0.99187 | 0.01670 | 0.00010 | 0.00003 |
| 4 | 0.14169 | −504.801 | −1.27367 | 203.206 | 0.99136 | 0.00098 | 0.00019 | 0.00006 |
| 5 | −0.02685 | 1.04813 | −0.82966 | 3.54796 | 0.98204 | 0.00288 | 0.00013 | 0.00004 |
| 6 | −0.01593 | 0.59991 | −0.80693 | 3.78710 | 0.99407 | 0.00103 | 0.00021 | 0.00007 |
| 7 | −0.01794 | 0.41420 | −0.62807 | 4.93334 | 0.98503 | 0.00265 | 0.00015 | 0.00005 |
| 8 | −0.08224 | −0.76052 | −1.01221 | 4.19428 | 0.98615 | 0.00258 | 0.00017 | 0.00008 |
| 9 | −0.56170 | −0.01057 | −1.00003 | 4.61364 | 0.99686 | 0.00149 | 0.00005 | 0.00001 |
| 10 | −0.04378 | −0.40158 | −0.95785 | 4.21470 | 0.98015 | 0.00367 | 0.00026 | 0.00009 |
| 11 | −0.00158 | 0.56974 | −0.68545 | 4.14182 | 0.98948 | 0.00220 | 0.00021 | 0.00008 |
| 12 | 0.01754 | −1.05718 | −1.01575 | 11.2206 | 0.99581 | 0.00187 | 0.00011 | 0.00003 |
| 13 | −0.03018 | 0.99844 | −0.80578 | 3.87855 | 0.98785 | 0.00219 | 0.00014 | 0.00005 |
| 14 | −0.02755 | 0.65861 | −0.76147 | 4.08546 | 0.98984 | 0.00389 | 0.00014 | 0.00003 |
| 15 | −0.02458 | 0.48597 | −0.57960 | 3.97585 | 0.99152 | 0.00184 | 0.00008 | 0.00002 |

The thermal decomposition kinetics were modified with the help of equations and the temperature-dependent functional equation of the conversion is obtained in Eq. (7). Using this equation, sample calculation with nonlinear regression was performed for experiment 3 (2 wt.%), and the data in Table 5 are obtained.

Kinetic and statistical parameters in Table 6 are found using the kinetic models in Table 3. In the calculations for experiment 3, the decomposition kinetics of the polyester composite were examined in three regions. In the first region (298–418 K), volatile components and physical impurities are separated from the structure by the effect of temperature. In the second region, chemical decomposition begins (418–718) and degradation is the fastest process. In the third region (718–918 K), thermal degradation slows down and the remaining cross-linked components move away from the structure. When Table 6 is examined considering experiment 3, the Midilli-Kucuk model stands out in the 1st, 2nd, and 3rd regions. Also, it is observed that the Modified Page model is dominant in the 1st and 2nd thermal degradation zones.

In Eq. (8), it can be solved by writing Arrhenius equation instead of *k(T)*. In this case, Eq. (9) is obtained according to Coats and Redfern method (Taylor series expansion was used) (Khawam and Flanagan 2006; Linghu et al. 2019).

$$k(T) = A \exp\left(-\frac{E}{RT}\right) \tag{8}$$

$$\ln \frac{g(\delta)}{T^2} = \ln \frac{AR}{\alpha E} - \frac{E}{RT} \tag{9}$$

The Arrhenius coefficients in Table 7 are found by applying Eq. (9) using the Coats-Redfern method. Activation energy ($E$) and Arrhenius constant ($A$) can

**Table 6.** Thermal decomposition kinetics and statistical analysis for experiment 3 (2 wt.%).

| Models | T (K) | k | a | B | C | $R^2$ | RMSE | SSE | $\chi^2$ |
|---|---|---|---|---|---|---|---|---|---|
| 1 | 298–418 | 0.00449 | | | | 0.95060 | 0.01284 | 0.00082 | 0.00041 |
| | 418–718 | 0.01601 | | | | 0.99509 | 0.05902 | 0.01742 | 0.00871 |
| | 718–918 | 0.05316 | | | | 0.85225 | 0.00836 | 0.00035 | 0.00017 |
| 2 | 298–418 | 0.00032 | | | 2.14780 | 0.99567 | 0.00374 | 0.00007 | 0.00004 |
| | 418–718 | 0.00024 | | | 2.28131 | 0.99153 | 0.02291 | 0.00262 | 0.00131 |
| | 718–918 | 0.78373 | | | 0.30300 | 0.83481 | 0.00160 | 0.00002 | 0.00001 |
| 3 | 298–418 | 0.03047 | | | 2.59947 | 0.99948 | 0.00055 | 0.00001 | 0.00000 |
| | 418–718 | 1.56625 | | | −0.2400 | 0.99620 | 0.09585 | 0.04594 | 0.02297 |
| | 718–918 | 0.44741 | | | 0.30300 | 0.83607 | 0.00160 | 0.00002 | 0.00001 |
| 4 | 298–418 | 0.00848 | 1.03629 | | | 0.94856 | 0.00542 | 0.00015 | 0.00007 |
| | 418–718 | 0.04722 | 2.24659 | | | 0.99611 | 0.00553 | 0.00015 | 0.00008 |
| | 718–918 | 0.01596 | 0.17109 | | | 0.82285 | 0.00165 | 0.00002 | 0.00001 |
| 5 | 298–418 | 0.00035 | 23.6294 | −22.5947 | | 0.95268 | 0.00520 | 0.00014 | 0.00007 |
| | 418–718 | 0.04406 | 2.22017 | −0.04765 | | 0.99613 | 0.00552 | 0.00015 | 0.00008 |
| | 718–918 | 1.10667 | 0.10667 | 0.07999 | | 0.80959 | 0.00395 | 0.00008 | 0.00004 |
| 6 | 298–418 | 0.00848 | 0.74213 | 0.29416 | 0.00847 | 0.94856 | 0.00542 | 0.00015 | 0.00007 |
| | 418–718 | 0.04712 | 0.24359 | 2.00302 | 0.04724 | 0.99611 | 0.00553 | 0.00015 | 0.00008 |
| | 718–918 | 0.01598 | 0.08564 | 0.08563 | 0.01599 | 0.82287 | 0.00165 | 0.00002 | 0.00001 |
| 7 | 298–418 | 0.00449 | 0.99972 | | | 0.95060 | 0.01284 | 0.00082 | 0.00041 |
| | 418–718 | 12.0867 | 0.00132 | | | 0.99509 | 0.05912 | 0.01747 | 0.00874 |
| | 718–918 | 0.05316 | 1.00018 | | | 0.85225 | 0.00836 | 0.00035 | 0.00017 |
| 8 | 298–418 | 6.62728 | 729.246 | −0.01174 | −0.0198 | 0.99555 | 0.00160 | 0.00002 | 0.00001 |
| | 418–718 | 0.14199 | 2.97922 | 0.69978 | −0.0033 | 0.99617 | 0.00549 | 0.00015 | 0.00008 |
| | 718–918 | 0.01707 | 2.64492 | 1.47396 | 0.00130 | 0.96947 | 0.00069 | 0.00001 | 0.00000 |
| 9 | 298–418 | 0.04260 | −45.422 | 0.97684 | | 0.99276 | 0.00205 | 0.00002 | 0.00001 |
| | 418–718 | 0.38092 | −1.2494 | 0.12408 | | 0.99611 | 0.00553 | 0.00015 | 0.00008 |
| | 718–918 | 0.73366 | 0.82863 | 0.02180 | | 0.82288 | 0.00165 | 0.00002 | 0.00001 |
| 10 | 298–418 | 0.33382 | −0.0551 | 0.01002 | | 0.97305 | 0.00396 | 0.00008 | 0.00004 |
| | 418–718 | 0.04722 | 2.24656 | 1.46245 | | 0.99611 | 0.00553 | 0.00015 | 0.00008 |
| | 718–918 | 1.49180 | 0.82891 | 0.01596 | | 0.82285 | 0.00165 | 0.00002 | 0.00001 |

**Table 7.** Kinetic parameters from (Coats and Redfern method) the thermal decomposition.

| | 0 wt.% | | | 2 wt.% | | | 4 wt.% | | |
|---|---|---|---|---|---|---|---|---|---|
| Numbers | A (1/min) | E (kJ/mol) | $R^2$ | A (1/min) | E (kJ/mol) | $R^2$ | A (1/min) | E (kJ/mol) | $R^2$ |
| 1 | 0.00002 | 10.5683 | 0.99302 | 0.00001 | 11.72632 | 0.96759 | 0.00001 | 13.23101 | 0.90626 |
| 2 | 0.00005 | 13.3568 | 0.99420 | 0.00004 | 15.96746 | 0.97704 | 0.00003 | 18.64052 | 0.91152 |
| 3 | 0.00010 | 16.2510 | 0.99443 | 0.00007 | 17.78803 | 0.97902 | 0.00006 | 19.69522 | 0.92112 |
| 4 | 0.00047 | 32.0185 | 0.92540 | 0.00043 | 34.11876 | 0.96197 | 0.00039 | 37.60040 | 0.99093 |
| 5 | 0.00135 | 38.3917 | 0.96474 | 0.00110 | 39.42442 | 0.98716 | 0.00093 | 41.67937 | 0.99859 |
| 6 | 0.00454 | 48.1001 | 0.99556 | 0.00273 | 50.55141 | 0.99882 | 0.00211 | 55.91930 | 0.98563 |
| 7 | 0.00071 | 41.4787 | 0.97934 | 0.00053 | 43.62296 | 0.99460 | 0.00043 | 48.83392 | 0.99740 |
| 8 | 0.00063 | 24.9337 | 0.99478 | 0.00040 | 28.24975 | 0.98201 | 0.00033 | 32.85934 | 0.93564 |
| 9 | 0.74299 | 49.9216 | 0.90691 | 0.15422 | 52.90225 | 0.92003 | 0.11345 | 59.89421 | 0.90318 |
| 10 | 8.68393 | 81.8671 | 0.90364 | 8.42235 | 83.83417 | 0.90812 | 6.92828 | 95.56025 | 0.89546 |
| 11 | 0.00023 | 32.0185 | 0.92540 | 0.00021 | 34.21876 | 0.96197 | 0.00020 | 37.60040 | 0.99093 |
| 12 | 0.00135 | 38.3917 | 0.96474 | 0.00110 | 41.42442 | 0.98716 | 0.00093 | 45.67937 | 0.99859 |
| 13 | 0.00681 | 48.1001 | 0.99556 | 0.00410 | 50.55141 | 0.99882 | 0.00316 | 56.91930 | 0.98563 |
| 14 | 9.93032 | 73.9740 | 0.97281 | 2.15575 | 76.84569 | 0.95339 | 1.39626 | 82.58102 | 0.89943 |
| 15 | 0.00002 | 27.4172 | 0.91385 | 0.00002 | 30.65952 | 0.94646 | 0.00002 | 34.86955 | 0.98371 |

be calculated from the slope and intercept of the $\ln[g(\delta)/T^2]$ with $1/T$ plot, respectively. When the activation energies in Table 7 are examined, it was seen that thermal decomposition slows down as the aerosil ratio by mass increases. According to the results in Table 7, it is seen that the three-dimensional diffusion and Jander equation functions are very compatible with the experimental

**Table 8.** Proximate analyses result of the unsaturated polyester and nanocomposites.

| Experiments | (%) Moisture | (%) Ash | (%) Other volatiles |
|---|---|---|---|
| 1 | 8.08 | 8.35 | 83.57 |
| 2 | 7.76 | 6.34 | 85.90 |
| 3 | 6.02 | 4.32 | 89.66 |
| 4 | 5.75 | 2.30 | 91.95 |
| 5 | 5.13 | 0.29 | 94.58 |

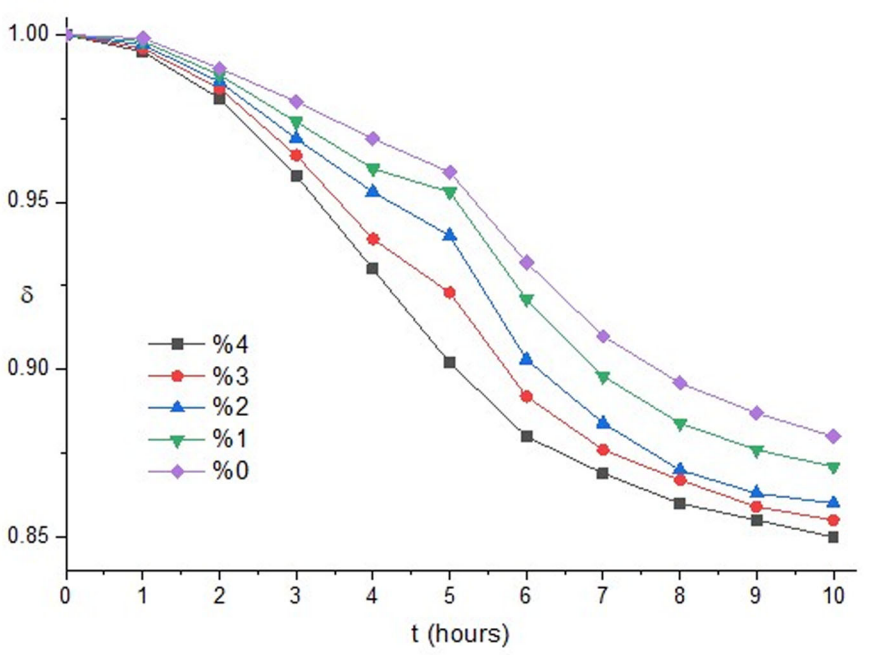


**Figure 2.** Drying behavior of the synthesized the unsaturated polyester and nanocomposites.

results for 3 with 5 experiments. In the Coats-Redfern method, the best results for the 1st experiment were found in the solution obtained with the two-dimensional diffusion and Holt-Cutler-Wadsword functions. In other words, the increase in the activation energy indicates that the thermal stability also increases (Vassiliou, Chrissafis and Bikiaris 2010).

The results obtained in the experimental studies in Table 8 express the percentage of moisture, ash, and other volatiles compositions of the polyester and polyester composites. Here, the amount of ash in polyester and composites is proportional to the amount of aerosil used in the experiments, because there was no thermal decomposition even at very high temperatures in aerosil 300.

In Figure 2, the drying process of the polymers at the temperature of 293 K was carried out in non-isothermal conditions with a temperature increase of 10 K/h in a total of 10 h. Physical impurities (such as moisture, solvent) in the structure of polyester and composites have been removed.

Thermal decomposition of polymers was carried out under non-isothermal conditions with a temperature increase of 10 K/min. In the thermal

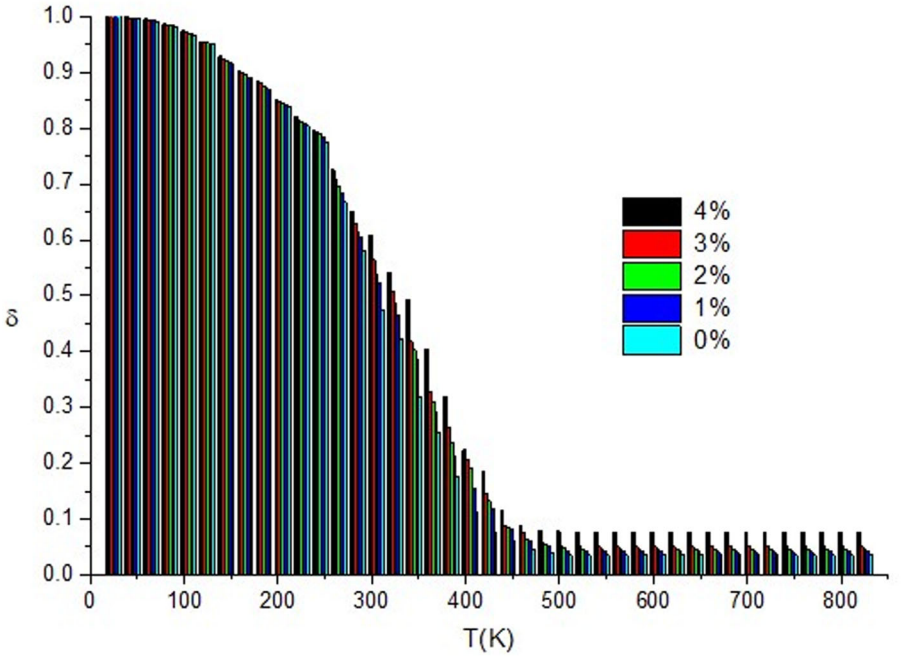


**Figure 3.** Thermal decomposition diagrams of the unsaturated polyester and nanocomposites.

decomposition kinetics of pure polyester and nanocomposites shown in Figure 3, the slowest sample is the polymer with 4 wt.% composition. In other words, the thermal stability of pure polyester is lower than nanocomposites (Li and Huang 1999).

In Figure 4, the thermal conductivity coefficients of pure polyester and nanocomposites were compared. It is a good insulating material because the density of nano-sized aerosil is very low, and its porosity, surface area, and temperature resistance are very high. For these reasons, the aerosil has improved both the thermal stability and the insulation properties of the polyester.

Figure 5 shows FTIR spectra of polyester and nanocomposite. Due to the aerosil in the nanocomposite, Si-O and Si-O-Si bonds are seen in the structure. The stretch vibration of OH groups is in the wavelength of 3,597 $cm^{-1}$, and C–H symmetric and asymmetric stress vibrations are seen in 2,964 and 2,896 $cm^{-1}$ wavelengths. Vibrations of carbonyl groups are seen at (C = O) 1,718 $cm^{-1}$ and (C-O) 1,134 $cm^{-1}$ wavelengths. A very large peak was observed at 1,718 $cm^{-1}$ due to the carbonyl (C = O) in the ester bonds. This indicates an esterification reaction between covalently bonded hydroxyl groups and polyester COOH groups. The double bonds in maleic structure in polyester are seen in FTIR spectrum at 1,636 $cm^{-1}$ wavelength. The peaks at 1,539 $cm^{-1}$ wavelength represent C = C stretching vibrations in the aromatic ring. Asymmetric stress vibrations of Si-O-Si bonds in the aerosil were observed at wavelengths at approximately

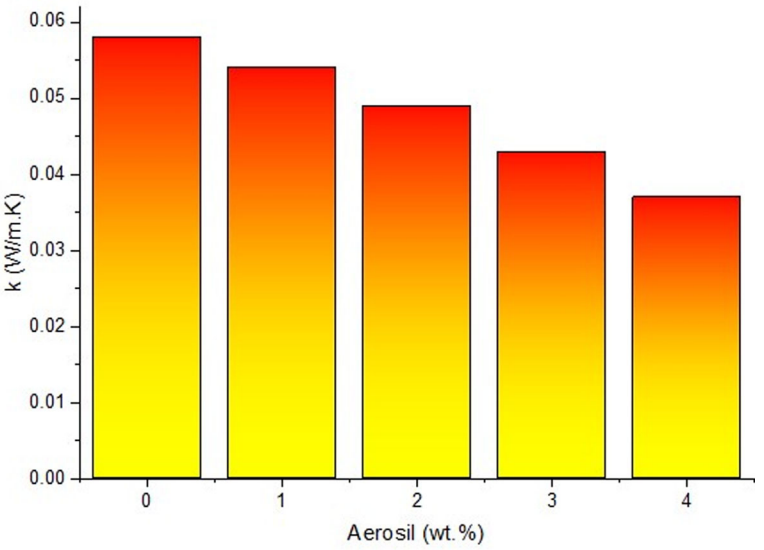


**Figure 4.** Thermal conductivity of the unsaturated polyester and nanocomposites.

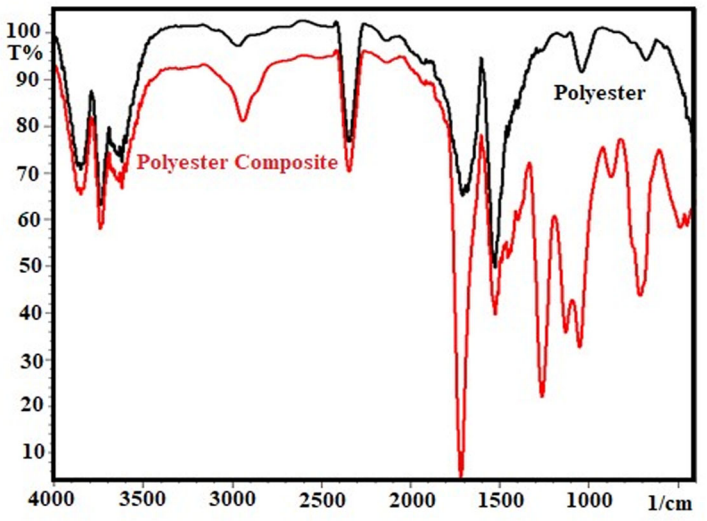


**Figure 5.** FTIR spectrum of the unsaturated polyester and nanocomposite (4 wt.%).

1,041 $cm^{-1}$. It also expresses the strain vibrations of Si-O at 853 $cm^{-1}$. Chemical bonds and wavelengths of the polyester and nanocomposites were expressed according to FTIR spectrum data in Table 9. FTIR spectra of the polyester and composites were made using the Shimadzu S11025C instrument (White, Catallo, and Legendre 2011).

Figures 6 and 7 show SEM images of pure polyester and nanocomposite (4 wt.%), respectively. The arrangement of nano-sized aerosil particles can be seen on the composite surface.

**Table 9.** FTIR spectrum analysis of the polyester and nanocomposite.

| Wavelength ($cm^{-1}$) | Bond structures formed |
|---|---|
| 3,597 | Stress vibration of the hydroxyl (OH) groups |
| 2,964 | C-H stretching vibrations |
| 2,896 | $CH_2$ groups of symmetrical stress vibrations of methylene |
| 1,718 | Carbonyl (C = O) groups |
| 1,636 | C = O maleic structure groups |
| 1,539 | C = C stretching of aromatic ring |
| 1,456 | CH3 asymmetric bending |
| 1,398 | CH3 symmetrical bending |
| 1,263 | CH2 bending |
| 1,134 | C-O stretching vibrations |
| 1,041 | Si-O-Si stretching vibrations |
| 853 | ≡Si-O- |
| 754 | ≡Si-O-O* Nanocluster |
| 677 | ≡Si-O* |


**Figure 6.** SEM image of unsaturated polyester.

## 4. Conclusions

It was observed that as the mass ratio of the aerosil additive went up, the density of the polyester composite obtained decreased. Nano-sized high-surface area aerosil particles reduced the thermal conductivity coefficient of polyester. In this case, it was determined that the isolation feature of the nanocomposite was improved. Because of its aerosil reinforcement, polyester composite has lower density, high thermal stability, and better thermal insulation, so it will be of great advantage to be used in many applications.

In the first region, the effect of temperature separates volatile components and physical impurities from the structure (298–418 K). In the second region, chemical decomposition (418–718) begins, with degradation being

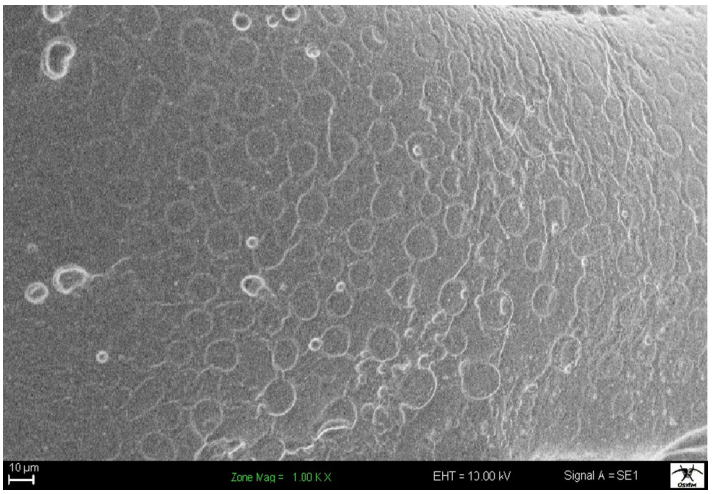


**Figure 7.** SEM image of polyester nanocomposite (4 wt.%).

the fastest step. The remaining cross-linked components move away from the structure as thermal degradation slows in the third region (718–918 K).

The second-order model was found to be the most suitable result in the thermal decomposition kinetics of polyester nanocomposites using the special mathematical solution (f $(\delta) = (1-\delta)^2$, E: 53.492 kJ/mol, $R^2$: 0.99686, $\chi^2$: $1{\cdot}10^{-5}$ for 2 wt.%). Besides, using the Coats-Redfern approach, better results were found with three-dimensional diffusion and Jander functions ($R^2$: 0.99882, E: 50.55141 kJ/mol for 2 wt.%). The Midilli and Kucuk model produced the most reliable results in drying kinetics of polyester nanocomposites ($R^2$: 0.99575, RMSE: 0.03099, SSE: 0.00267, $\chi^2$: 0.00036 for 4 wt.%). When the thermal decomposition of polyester composites was compared with kinetic models in three regions, the Modified Page model in the first and second regions, and the Midilli and Kucuk models in the third region, produced the most consistent theoretical results with the experimental data.

## Nomenclature

| | |
|---|---|
| $R^2$ | coefficient of determination |
| SEE | standard error of estimate |
| SST | total sum of squares |
| SSR | residual sum of squares |
| $\chi^2$ | chi square |
| RMSE | root mean square error |
| TGA | thermogravimetric analysis |
| FTIR | Fourier transform infrared spectrophotometer |
| MEKP | methyl ethyl ketone peroxide |
| E | activation energy |
| A | Arrhenius constant |

## References


Al-Mulla, A., J. Mathew, L. Al-Omairi, and S. Bhattacharya. 2011. Thermal decomposition kinetics of tricomponent polyester/polycarbonate systems. *Polymer Engineering and Science* 51 (11):2335–2344.

Alameri, I., and M. Oltulu. 2020. Mechanical properties of polymer composites reinforced by silica-based materials of various sizes. *Applied Nanoscience* 10 (11):4087–4102. doi: 10.1007/s13204-020-01516-6.

Ahmad, T., S. S. Raza, E. Aleem, M. Kamran, U. Manzoor, A. Makhdoom, R. Ahmad, and S. Mukhtar. 2017. Improvement in mechanical and thermal properties of unsaturated polyester- based hybrid composites. *Iranian Polymer Journal* 26 (4):305–311. doi: 10.1007/s13726-017-0520-6.

Badía, J. D., L. Santonja-Blasco, R. Moriana, and A. Ribes-Greus. 2010. Thermal analysis applied to the characterization of degradation in soil of polylactide: II. On the thermal stability and thermal decomposition kinetics. *Polymer Degradation and Stability* 95 (11): 2192–2199. doi: 10.1016/j.polymdegradstab.2010.06.002.

Chrissafis, K., E. Roumeli, K. M. Paraskevopoulos, N. Nianias, and D. N. Bikiaris. 2012. Effect of different nanoparticles on thermal decomposition of poly (propylene sebacate)/ nanocomposites: Evaluation of mechanisms using TGA and TG–FTIR–GC/MS. *Journal of Analytical and Applied Pyrolysis* 96:92–99. doi: 10.1016/j.jaap.2012.03.010.

Halim, Z. A. A., M. A. M. Yajid, F. A. Nurhadi, N. Ahmad, and H. Hamdan. 2020. Effect of silica aerogel – Aluminium trihydroxide hybrid filler on the physio-mechanical and thermal decomposition behaviour of unsaturated polyester resin composite. *Polymer Degradation and Stability* 182:109377. doi: 10.1016/j.polymdegradstab.2020.109377.

Hayoune, F., S. Chelouche, D. Trache, S. Zitouni, and Y. Grohens. 2020. Thermal decomposition kinetics and lifetime prediction of a PP/PLA blend supplemented with iron stearate during artificial aging. *Thermochimica Acta* 690:178700. doi: 10.1016/j.tca.2020.178700.

Majeed, A. H., and Ibrahim, S. Q. 2017. Mechanical properties of unsaturated polyester filled with silica fume, glass powder and carbon black. *Engineering and Technology Journal* 35 (6).

Khawam, A., and D. R. Flanagan. 2006. Solid-state kinetic models: Basics and mathematical fundamentals. *The Journal of Physical Chemistry B* 110 (35):17315–17328. doi: 10.1021/jp062746a.

Kucharek, M., W. MacRae, and L. Yang. 2020. Investigation of the effects of silica aerogel particles on thermal and mechanical properties of epoxy composites. *Composites Part A Applied Science and Manufacturing* 139:106108. doi: 10.1016/j.compositesa.2020.106108.

Levchik, S. V., and E. D. A. Weil. 2004. Review on thermal decomposition and combustion of thermoplastic polyesters. *Polymers for Advanced Technologies* 15 (12):691–700. doi: 10.1002/pat.526.

Li, X. G., and M. R. Huang. 1999. Thermal decomposition kinetics of thermotropic poly(oxybenzoate-co-oxynaphthoate) Vectra copolyester. *Polymer Degradation and Stability* 64 (1):81–90. doi: 10.1016/S0141-3910(98)00175-X.

Li, Y., Z. Qiang, X. Chena, and J. Ren. 2019. Understanding thermal decomposition kinetics of flame-retardant thermoset polylactic acid. *Royal Society of Chemistry* 9:3128.

Linghu, R., Y. Zhang, M. Zhao, L. Huang, G. Sun, and S. Zhang. 2019. Combustion reaction kinetics of char from in-situ or ex-situ pyrolysis of oil shale. *Estonian Academy Publishers* 36 (3):392–409.

Majeed, A. H. 2018. Enforcement of epoxy with silica fume and carbon fiber. *Tikrit Journal of Engineering Sciences* 25 (1):74–7.

Mourad, A. H. I., B. Abu-Jdayil, and M. Hassan. 2020. Mechanical behavior of Emirati red shale fillers/unsaturated polyester composite. *SN Applied Sciences* 2 (3):1–9. doi: 10.1007/s42452-020-2284-4.

Ott, R. L., and M. Longnecker. 2001. *An introduction to statistical methods and data analysis*. 1–1213, 5th ed. USA: Duxbury, Cengage Learning, Wadsworth Group.

Phogat, V., M. A. Skewes, J. W. Cox, and J. Simunek. 2016. Statistical assessment of a numerical model simulating agro hydro-chemical processes in soil under drip fertigated mandarin tree. *Irrigation and Drainage Systems Engineering* 5 (1):1000155.

Rajaee, P., F. Ashenai Ghasemi, M. Fasihi, and M. Saberian. 2019. Effect of styrene-butadiene rubber and fumed silica nano-filler on the microstructure and mechanical properties of glass fiber reinforced unsaturated polyester resin. *Composites Part B: Engineering* 173: 106803. doi: 10.1016/j.compositesb.2019.05.014.

Singh, G., H. Kumar, and S. Singh. 2019. Performance evaluation-PET resin composite composed of red mud, fly ash and silica fume. *Construction and Building Materials* 214: 527–38. doi: 10.1016/j.conbuildmat.2019.04.127.

Singh, A., R. Kumar, P. K. Soni, and V. Singh. 2020. Compatibility and thermal decomposition kinetics between HMX and some polyester-based polyurethanes. *Journal of Thermal Analysis and Calorimetry* 5:09377.

Terzopoulou, Z., E. Tarani, N. Kasmi, L. Papadopoulos, K. Chrissafis, D. G. Papageorgiou, G. Z. Papageorgiou, and D. N. Bikiaris. 2019. Thermal decomposition kinetics and mechanism of in-situ prepared bio-based poly(propylene 2,5-furan dicarboxylate)/graphene nanocomposites. *Molecules* 24 (9):1717. doi: 10.3390/molecules24091717.

Terzopoulou, Z., V. Tsanaktsis, M. Nerantzaki, D. S. Achilias, T. Vaimakis, G. Z. Papageorgiou, and D. N. Bikiaris. 2016. Thermal degradation of biobased polyesters: Kinetics and decomposition mechanism of polyesters from 2,5-furandicarboxylic acid and long-chain aliphatic diols. *Journal of Analytical and Applied Pyrolysis* 117:162–175. doi: 10.1016/j.jaap.2015.11.016.

Tibiletti, L., C. Longuet, L. Ferry, P. Coutelen, A. Mas, J.-J. Robin, and J.-M. Lopez-Cuesta. 2011. Thermal degradation and fire behaviour of unsaturated polyesters filled with metallic oxides. *Polymer Degradation and Stability* 96 (1):67–75. doi: 10.1016/j.polymdegradstab.2010.10.015.

TranVan, L., V. Legrand, and F. Jacquemin. 2014. Thermal decomposition kinetics of balsa wood: Kinetics and degradation mechanisms comparison between dry and moisturized materials. *Polymer Degradation and Stability* 110:208–215. doi: 10.1016/j.polymdegradstab.2014.09.004.

Tsanaktsis, V., E. Vouvoudi, G. Z. Papageorgiou, D. G. Papageorgiou, K. Chrissafis, and D. N. Bikiaris. 2015. Thermal degradation kinetics and decomposition mechanism of polyesters based on 2,5-furandicarboxylic acid and low molecular weight aliphatic diols. *Journal of Analytical and Applied Pyrolysis* 112:369–378. doi: 10.1016/j.jaap.2014.12.016.

Vassiliou, A. A., K. Chrissafis, and D. N. Bikiaris. 2010. In situ prepared PET nanocomposites: Effect of organically modified montmorillonite and fumed silica nanoparticles on PET physical properties and thermal degradation kinetics. *Thermochimica Acta* 500 (1–2):21–29. doi: 10.1016/j.tca.2009.12.005.

White, J. E., W. J. Catallo, and B. L. Legendre. 2011. Biomass pyrolysis kinetics: A comparative critical review with relevant agricultural residue case studies. *Journal of Analytical and Applied Pyrolysis* 91 (1):1–33. doi: 10.1016/j.jaap.2011.01.004.